TISSUE ENGINEERING: Part C
Volume 19, Number 5, 2013

DOI: 10.1089/ten.tec.2012.0467

Characterizing Morphology and Nonlinear Elastic Properties of Normal and Thermally Stressed Engineered Oral Mucosal Tissues Using Scanning Acoustic Microscopy

Frank Winterroth, PhD,[1] Kyle W. Hollman, PhD,[1,2] Shiuhyang Kuo, DDS, PhD,[3] Arindam Ganguly, PhD,[4] Stephen E. Feinberg, DDS, PhD,[1,3] J. Brian Fowlkes, PhD,[1,5] and Scott J. Hollister, PhD[1,6]

This study examines the use of high-resolution ultrasound to monitor changes in the morphology and nonlinear elastic properties of engineered oral mucosal tissues under normal and thermally stressed culture conditions. Nonlinear elastic properties were determined by first developing strain maps from acoustic ultrasound, followed by fitting of nonlinear stress–strain data to a 1-term Ogden model. Testing examined a clinically developed *ex vivo* produced oral mucosa equivalent (EVPOME). As seeded cells proliferate on an EVPOME surface, they produce a keratinized protective upper layer that fills in and smoothens out surface irregularities. These transformations can also alter the nonlinear stress/strain parameters as EVPOME cells differentiate. This EVPOME behavior is similar to those of natural oral mucosal tissues and in contrast to an unseeded scaffold. If ultrasonic monitoring could be developed, then tissue cultivation could be adjusted in-process to account for biological variations in their development of the stratified cellular layer. In addition to ultrasonic testing, an in-house-built compression system capable of accurate measurements on small ($\sim$1.0–1.5 cm^2) tissue samples is presented. Results showed a near 2.5-fold difference in the stiffness properties between the unstressed EVPOME and the noncell-seeded acellular scaffold (AlloDerm®). There were also 4$\times$greater differences in root mean square values of the thickness in the unseeded AlloDerm compared to the mature unstressed EVPOME; this is a strong indicator for quantifying surface roughness.

Introduction

There is a significant need for soft tissue replacements of oral mucosa in cases of disease, injury, or defect. Hence, developing a practical and cost–effective engineered tissue device is essential toward proper treatment of soft tissue conditions. This study examines using scanning acoustic microscopy (SAM) as a tool to study the morphology and nonlinear elastic characteristics of engineered oral mucosal tissues. The advantages of using SAM over conventional optical and electron microscopy include being able to image cells and tissues without doing any preparations that could potentially kill or alter these tissues; this provides a more accurate representation of the tissues' properties.[1,2,20] We used SAM and an in-house-built mechanical compressor to examine the morphology and nonlinear elastic properties, specifically Ogden nonlinear elastic stress–strain models, respectively, of the commercially available acellular cadaveric dermis, AlloDerm® (LifeCell Corp.) and an in-house-designed *ex vivo* produced oral mucosa equivalent (EVPOME).

Seeded cell proliferation on the EVPOME device changes both the morphological and nonlinear elastic characteristics of the device. Specifically, as seeded cells proliferate, they fill in any surface irregularities, followed by producing a keratinized protective upper layer that smoothes out any remaining surface irregularities. This cellular activity will cause the morphological and nonlinear elastic properties of the engineered oral mucosa to continually evolve from the AlloDerm baseline to properties that represent mature, fully functional EVPOME. Therefore, the ability to characterize the morphological and nonlinear elastic characteristics of EVPOME in various stages of development would provide quality control for EVPOME. Using SAM, we show significant differences in both the surface profilometry [determined by first finding the instance of threshold value, fitting and subtracting the planar surface, and then calculating root-mean-squared (RMS) height] and the nonlinear stress strain behavior when comparing the EVPOME to the AlloDerm. Furthermore, we demonstrate that the nonlinear elastic properties, as characterized by a 1-term Ogden model, vary significantly between

[1]Department of Biomedical Engineering, University of Michigan, Ann Arbor, Michigan.
[2]Soundsight Research, Livonia, Michigan.
Departments of [3]Oral and Maxillofacial Surgery, [4]Chemistry, [5]Radiology, and [6]Surgery, University of Michigan, Ann Arbor, Michigan.

AlloDerm, fully functional EVPOME, and thermally stressed EVPOME that failed to properly develop. These results support the use of the SAM's ability to simultaneously characterize morphological and mechanical properties as a quality control methodology for engineered oral mucosa, and likely for general engineered soft tissues.[21,23]

Development and use of EVPOME have demonstrated its clinical efficacy in intraoral surgical grafts,[3,4] namely, as a clinically effective means of ensuring regeneration of oral mucosal tissues. In addition, oral mucosa tissues have been clinically reported to be a suitable transplant to treat vaginal agenesis.[5] Oral mucosa's histology resembles that of skin: as new cells are formed on the basal lamina, more matured cells migrate toward the apex, undergoing apoptosis and keratinization as they migrate[4]; this same process occurs in EVPOME tissues. What is still unknown is EVPOME's effectiveness as a functional replacement for other soft tissues such as dermal, vaginal, or urethral, as these tissues exhibit a nonlinear elastic mechanical behavior during physiologic function. Although the oral mucosa's histology resembles that of human epidermis and both tissue types are derived from ectodermal tissues, similarities in their physical properties have yet to be compared.

Although SAM has been used to study the morphology and density of skin tissue under both normal and pathological conditions,[6] it has not been applied toward understanding its nonlinear elastic properties. Further, no studies have yet examined the elastic parameters of oral tissues, either natural or engineered.

We have previously used SAM to compare changes in the radiofrequency (RF) data to EVPOME and natural oral mucosal tissues when they undergo differentiation and keratinization.[7] The spectral analysis results from SAM can be compared to histological images of the EVPOME tissues at different stages of growth and development. By correlating changes in the RF data to the EVPOME (and mucosal cells in general) undergoing differentiation, apoptosis,[15,16] and keratinization, we can better understand the physiological processes of these cells as they evolve.

Materials and Methods

The soft tissue compression set-up is derived from the experiments originally performed by Erkamp,[8] in which a cylindrical sample was indented while mounted on top of a glass slide. The system to measure the nonlinear elastic behavior of soft tissue is an in-house-built compressor using a cylindrical piston of known length and volume to indent the tissue sample at steps of a known length, registering as a change in mass (in grams) on an electronic scale (Ohaus Scout Pro). This compressor setup is illustrated in Figure 1a and b. The tissue sample is cylindrical in shape with an area (A) slightly larger than that of the piston. The piston is mounted directly over the center of the sample and pushes on the sample, producing a known amount of force. This force plus knowing the degree of surface displacement provide the nonlinear geometric stiffness characteristic for the given samples.

The gram-to-Newton force conversion was applied to obtain the appropriate force for each step using the following equation:

$$F = [(gr/1000)^{*}9.80665] \quad (1)$$

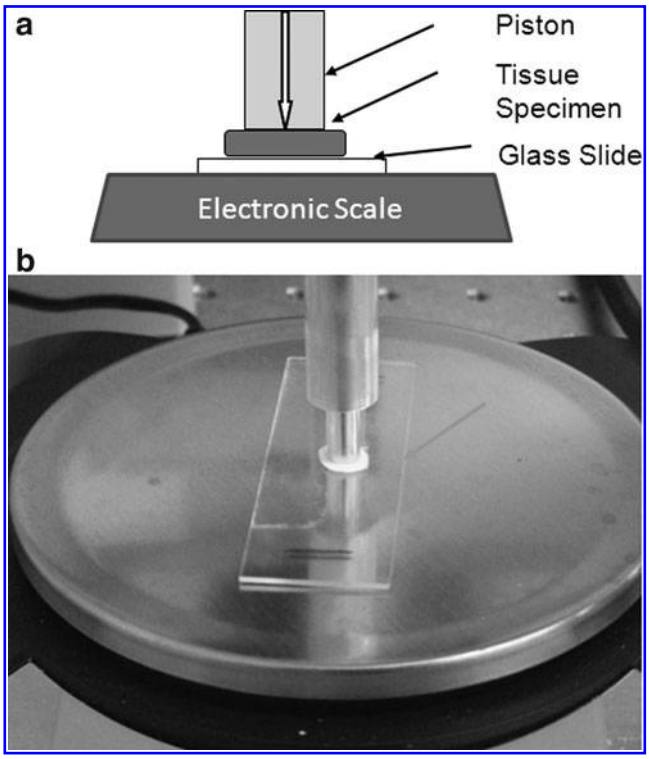

FIG. 1. **(a)** Schematic side view of the compression system used to measure indentation of soft tissue samples. The large white arrow shows the motion direction of the piston. **(b)** Photograph of the compression system testing a tissue specimen placed on top of a glass slide (arrow). The diameter of the compression piston is 1.0 cm.

where gr is the piston load in grams registered by the scale. For nonlinear elastic analysis, the compressive stress and deformation were measured. The stress measure is the 1st Piola-Kirchoff stress T defined as the current measured force divided by the original specimen area A:

$$T = F/A' \quad (2)$$

where the current force F is defined by equation 1, and A′ is the area of the specimens before deformation. The stretch ratio λ is simply defined as the deformed height of the specimen l divided by the original height of the specimen l′ as $\lambda = l/l'$. We further assume that the tissue is incompressible; that is, the tissue volume does not change during deformation. Since the deformation gradient tensor F_{ij} only has diagonal stretch ratios λ_1, λ_2, and λ_3 under the applied deformation, this implies that $\lambda_1\lambda_2\lambda_3 = 1$. The deformation is applied in the z (3) direction, and we further assume that the stretch ratios in the 2 and 3 direction are equal and due to incompressibility are related to λ_3 by the following expression:

$$\lambda_1 = \sqrt{\frac{1}{\lambda_3}} \quad (3)$$

A nonlinear elastic material is characterized using a strain energy function. We utilized a 1-term Ogden strain energy function to characterize the nonlinear elastic behavior of the

engineered oral mucosa. The 1-term Ogden strain energy model has two material constants μ and α:

$$W = \frac{\mu}{\alpha}(\lambda_1^{\alpha} + \lambda_2^{\alpha} + \lambda_3^{\alpha} - 3) \quad (4)$$

where λ_1, λ_2, and λ_3 are the stretch ratios' three Cartesian coordinate axes. Assuming incompressibility, the 1st Piola-Kirchoff stress in the z (3) direction may be calculated from the Ogden strain energy function as following:

$$T_{33} = -\frac{1}{\lambda_3}p + \frac{\partial W}{\partial \lambda_3} = -\frac{1}{\lambda_3}p + \mu\lambda_3^{\alpha-1} \quad (5)$$

where p is the hydrostatic pressure; T_{33} is the zz component of the 1st Piola-Kirchoff stress tensor; λ_3 is the stretch ratio in the 3 (z) direction; and W is the Ogden strain energy function from Equation. 3. Given the fact that the two faces of the test specimen are traction free, we can solve for the hydrostatic pressure p. Using this result with the relationship among stretch ratios due to incompressibility gives us the final relationship between the T_{33} 1st Piola-Kirchoff stress component, the μ and α coefficients from the Ogden strain energy function, and the stretch ratio λ_3; the final Ogden stress–strain produced is the following:

$$T_{33} = \mu\left(\lambda_3^{\alpha-1} - \lambda_3^{-\frac{1}{2}\alpha-\frac{1}{2}}\right) \quad (6)$$

The in-house SAM system has previously been used to obtain elastic properties—specifically, stress—strain parameters, and consequently, Young's modulus (correlates stress–strain to examine stiffness properties in the specimens) in different soft tissues, including porcine cornea.[9,10] The SAM's transducer parameters are a lateral resolution (R_{lat}) of 37 μm; an axial resolution (R_{ax}) of 24 μm; and a depth of field of 223 μm. The Z-axis was sampled at 300 megasamples/second. The R_{ax} is in the direction of propagation and is determined by the length of the ultrasound pulse propagating in the tissue; R_{lat} is orthogonal to the propagation direction of the ultrasound wave.

The nonlinear elastic properties of AlloDerm and other commercially available graft materials have been previously determined using a Fung strain energy function.[11,17–19] However, there are no known studies that have examined both the nonlinear elastic properties using an Ogden model and morphology of either AlloDerm or engineered mucosal tissues.

For this study, we examined the morphology and nonlinear elastic properties of engineered oral tissues using the SAM, followed by testing their mechanical properties using the cylindrical compressor. The last set of AlloDerm and EVPOME experiments involved mechanical compression studies on nonstressed and thermally stressed specimens of the aforementioned tissue types, the preparation, and examination being similar to our previous study.[12,22]

Methods for preparing both AlloDerm and EVPOME devices are similar to those described elsewhere.[13] Briefly, oral mucosa keratinocytes were enzymatically dissociated from the tissue sample, and a primary cell culture was established and propagated in a chemically defined, serum- and xenogenic product-free culture medium, with a calcium concentration of 0.06 mM. The AlloDerm specimens were soaked in 5 μg/cm^2 human type IV collagen overnight at 4°C before seeding cells to assist the adherence of cells, and then $\sim 2.0 \times 10^5$ cells/cm^2 of oral keratinocytes (cell lines: DPG3, JXP2) were seeded onto the type IV collagen-presoaked AlloDerm and cultured in a medium with 1.2 mM calcium. Morphologies of the unseeded AlloDerm® and the EVPOME at 11 days post-seeding are shown in Fig. 2. The composites of keratinocytes and AlloDerm were then cultured, in the submerged condition, for 4 days to form a continuous epithelial monolayer. At 4 days, samples of the EVPOME were collected while in the submerged condition for SAM imaging. After 4 days, the equivalents were raised to an air–liquid interface to encourage epithelial stratification and cultured for another 10 days, resulting in a fully differentiated, well-stratified epithelial layer on the AlloDerm. Unseeded AlloDerm specimens (used as controls) were subsequently treated in the same manner as EVPOMEs with the exception that they were never seeded with oral keratinocytes.

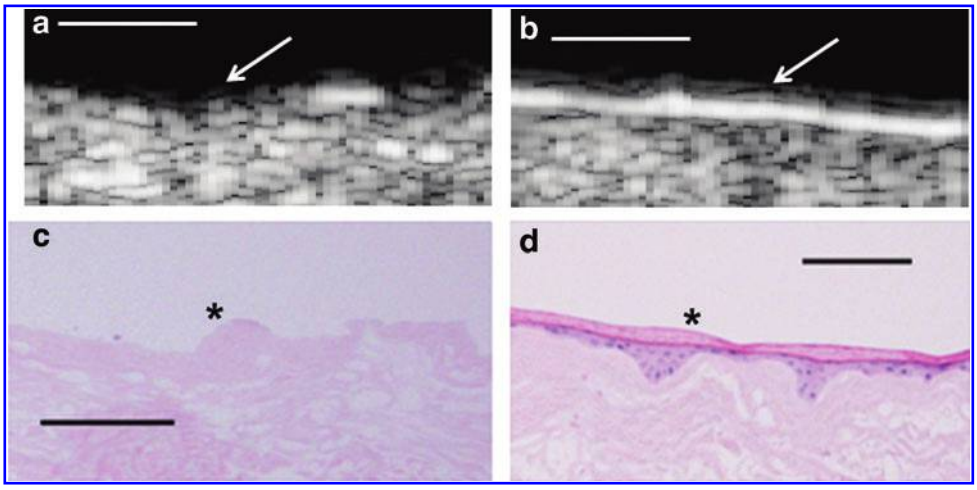

FIG. 2. **(a–d)** SAM 2D B-scans between the unseeded AlloDerm® scaffold **(a)** and the *ex vivo* produced oral mucosa equivalent (EVPOME) 11 days postseeding **(b)**, followed by their histological counterparts **(c** and **d)**. In the 2D B-scans, there is a greater reflectivity off of the surface of the EVPOME compared to the AlloDerm specimen (arrows), indicative of the space-filling/keratinization activity of the oral keratinocytes which were seeded onto its surface. This is verified in the histological micrograph comparing the two specimens (asterisk). Scale bars equal 100 μm. Color images available online at www.liebertpub.com/tec

For the last set of experiments, two additional AlloDerm and EVPOME specimens were prepared; these were then thermally stressed. For thermally stressed AlloDerm and EVPOME specimens, on Day 9 postseeding, one of each specimen was incubated at 43°C for 24 h, and then switched back to 37°C for another 24 h. Total incubation times were equal for all specimens. The purpose of thermal stressing is to simulate aberrant culture conditions that adversely affect development of the engineered oral mucosal tissue. There were two specimens each for all four of the aforementioned AlloDerm and EVPOME categories.

Details for the setup of the SAM have been detailed previously.[1,9,10] Briefly, AlloDerm and EVPOME samples were immersed in deionized water and imaged with a single-element fixed-focus transducer, producing ultrasonic B-scans. The transducer has an approximate frequency of 50 MHz, and the element is 3 mm in diameter and focused to a depth of 4.1 mm, giving an f/number of ~1.4. The transducer was fastened to an optical mount, and the angular position was adjusted until the ultrasonic beam was normal to a deflecting plate. We scanned surfaces of EVPOME and AlloDerm, showing the acoustic signal between the interface of the sample and water on each specimen's apical side. DC stepper motors positioned the transducer above the specimen. B-scan images were obtained by stepping the transducer element laterally across each desired region. At each position, the transducer fired, and an RF A-line was recorded. After repeated firings at one position, the transducer moved to the next position, where an image was constructed from A-lines acquired at all lateral positions. Because of low f/number, single-element transducers have a short depth of field; a composite B-scan image was generated from multiple scans at different heights. The SAM set up is illustrated in Figure 1 both as a schematic illustration (Fig. 1a) and a photograph (Fig. 1b), with differences in the acoustic patterns as they reflect off of the tissue boundaries (surface and base),[10,14] including the phase shift in sound waves when reflecting off tissue as opposed to the base surface of the holder, reflections off the surface and bottom of the tissue, and the sound speed through water and tissue. The tissue surface was determined by thresholding the magnitude of the signal at the first axial incidence of a value safely above noise, ~20–30 dB. All tissue specimens were imaged by SAM before and after compression testing by the cylinder compressor. 2D B-scan images of EVPOME and unseeded AlloDerm are shown in Figure 2a and b, along with their histology counterparts (Fig. 2c, d).

Further, 3D scans were produced as composites of the 2D B-scans for both AlloDerm and EVPOME (11 days postseeding) specimens. The threshold of the ultrasound signal was rendered as a dark surface; everything above the threshold was rendered in grayscale, and everything below was transparent (Fig. 3a, b). This was to better visualize surface characteristics of both tissue specimens.

Compression testing was performed on both unseeded AlloDerm and EVPOME (11 days postseeding) specimens by removing each specimen from an aqueous environment, measuring their thickness with an electronic caliper (Mituyo Corp.) and placing it under an in-house-built compression unit with cylindrical pistons which were either 540 mm^2 or 28.26 mm^2 in area. We used cylinders of varying sizes based on the size and the shape of the tissue specimens, in particular to perform multiple measurements at different locations on the tissues. A digital scale was placed directly beneath the specimen, tare to the weight of the specimen, and recorded changes in the weight for each successive step (10 μm) applied to the specimen by the piston. Further details of the mechanical setup and its applications and calculations are described under the Introduction section and illustrated in Figure 1. All stress levels were measured as kilopascals in relation to strain levels of the known compression step length.

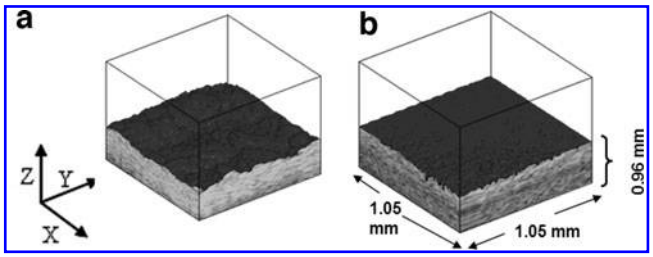

FIG. 3. SAM 3D composites of AlloDerm **(a)** and EVPOME at 11 days postseeding **(b)**, including the dimensions of the scanned region.

Both one-way analyses of variance (ANOVA) and linear regression analyses were performed to determine the RMS values for individual specimens. Mathematical fitting models of tissues (stressed and unstressed AlloDerm and 11 days postseeding EVPOME specimens), specifically 1-term Ogden models, were performed and analyzed using an algorithm running in MatLab (MathWorks, Inc.).

Results

In SAM 2D B-scans for AlloDerm and EVPOME devices, the transducer is positioned at the top of the image, pointing downward. Top bright echoes indicate the boundary between the coupling medium (water) and the apical surface of the AlloDerm. Below this, the tissue device appears as uniform speckle. Typical of speckle bright spots indicate phase aligned clusters of backscatter and are approximately 30 μm in diameter as expected from theses transducer characteristics. Post-compression RMS values between AlloDerm and EVPOME (11 days postseeding) are similar to those in previous studies where they were not subjected to compression: there is a significantly higher value (up to 4×greater) in the AlloDerm specimens than their EVPOME counterparts (Fig. 4).

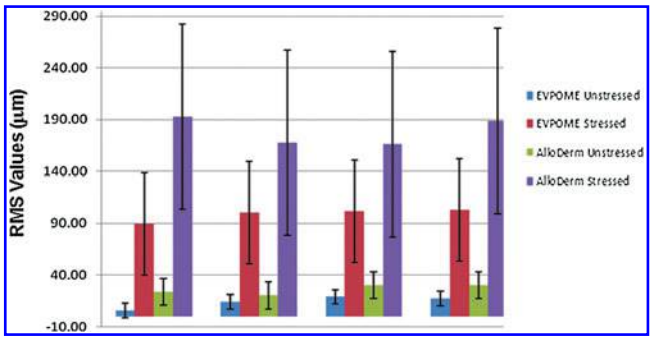

FIG. 4. Surface roughness (root-mean-squared (RMS) value) comparisons between unstressed and stressed EVPOME at 11 days postseeding and unstressed and stressed AlloDerm. Color images available online at www.liebertpub.com/tec

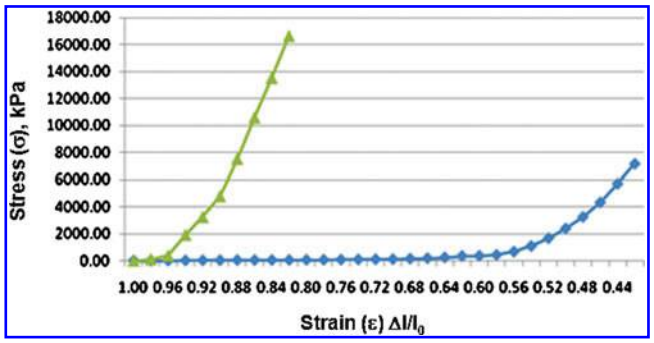

FIG. 5. Stress–strain relationships comparing AlloDerm® (green line) and EVPOME (blue line). Results optioned from direct mechanical piston measurements using equipment shown in Figure 1. Color images available online at www.liebertpub.com/tec

The AlloDerm specimen from the first compression tests was not subjected to any water exposure; that is, it was placed directly from a dry environment to the mechanical compression. For the second compression tests, it was immersed in a container of deionized water for ~10 min before testing. In all tests—both dry and wet—the unseeded AlloDerm specimens all exhibited significantly greater force with each successive step from the cylinder (Fig. 5), an indication of significant nonlinearity in the behavior of the unseeded scaffolds.

There were high variations in surface roughness as characterized by RMS values for the AlloDerm specimens—both stressed and unstressed—and for the stressed EVPOME specimen (Fig. 4). Such variations are clearly visible on the SAM B-Scans (Fig. 6a, b) and their histology images (Fig. 6c, d) for these specimens.

The AlloDerm Ogden coefficients for the thermally stressed and unstressed specimens were the same (stressed: $\mu = 4.77$ KPa, $\alpha = 4.8$; unstressed: $\mu = 4.77$ KPa, $\alpha = 4.8$), indicating that thermally stressing the AlloDerm does not change its nonlinear elastic properties. The EVPOME Ogden coefficients differed significantly between stressed ($\mu = 0.22$ KPa, $\alpha = 9.9$) and unstressed specimens ($\mu = 1.99$ KPa, $\alpha = 3.4$). All data were fit well by the Ogden model ($R^2 > 0.96$ for all fits) (Fig. 7); μ and α are material constants. The unstressed EVPOME appeared to be actually closer to the nonlinear mechanics of the AlloDerm. A compendium of the stress–strain comparisons among the EVPOME (both unstressed and stressed), AlloDerm (both unstressed and stressed) is seen in Table 1.

Discussion

Comparing unseeded AlloDerm specimens to engineered oral mucosal tissues (EVPOME) using acoustic imaging, we have seen major differences on surface characteristics of their reflectivity between unseeded device and mature EVPOME.[7] In this study, we show that the presence of cells (particularly in a stratified pattern) provides changes not only in the reflectivity of the cells, but also in their nonlinear elastic properties. Even the minimal presences of cells—including seeded layers that are rather poorly developed—still demonstrate resistance to stress at increasing strain deformations.

Because of the tissues' incompressibility, the change in volume remains essentially constant; this is likely due to their high water content, particularly the tissues within the oral cavity. The μ coefficient reflects the initial stiffness (lower values indicating lower stiffness), while the α exponent reflects the transition to stiffening with increasing deformation. Thus, the values for EVPOME indicate that stressed EVPOME is initially much compliant than unstressed EVPOME, and undergoes a much more rapid transition to stiffening behavior. Both EVPOME constructs are initially more compliant than AlloDerm, but the stressed EVPOME shows a much more rapid transition to stiffening behavior than either unstressed EVPOME or AlloDerm condition. These nonlinear property differences reflect the significant changes in mechanical function due to presence of oral keratinocytes and the quality of the extracellular matrix produced by these cells. It is important to note that the use of linear mechanical constitutive models (i.e., Hooke's law) would not reflect changes in function, as a linear model would have to be fit to either the initial or stiffened portion of the nonlinear stress–strain curve.

The amount of stratified cell layers within tissue types appears to play a significant role in the degree of stiffness each tissue displays; this is evident in the low stress–strain

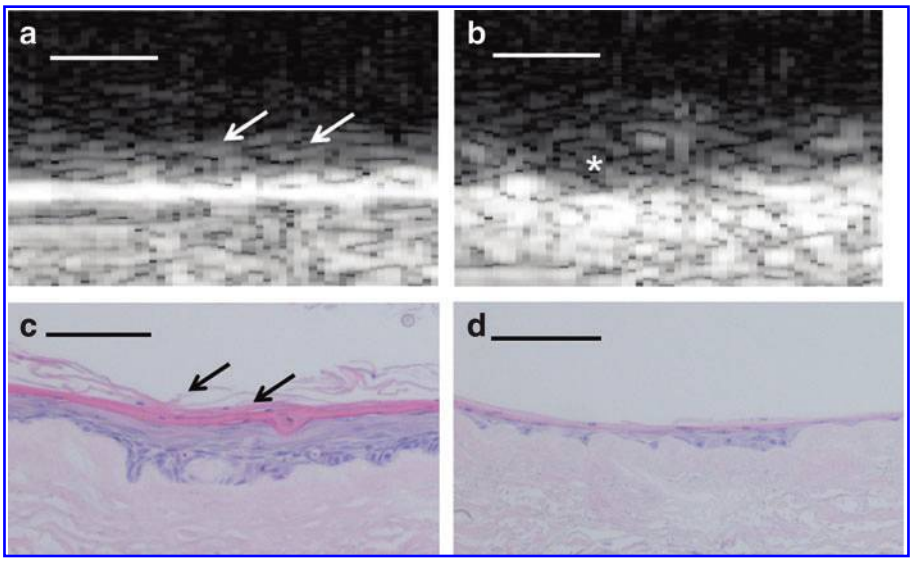

FIG. 6. **(a–d)** Comparative 2D B-scans **(a, b)** and histology **(c, d)** images between EVPOME (11 days postseeding) that was properly developed and keratinized **(a** and **c)** EVPOME that was poorly evolved and differentiated **(b** and **d)**. The keratin levels in the properly developed specimens are significantly greater in the staining and reflectivity (arrows). The lower acoustic reflection in the surface of the poorly developed EVPOME is a result of the reduced keratin layer on the surface (asterisk). Scale bars equal 100 μm. Color images available online at www.liebertpub.com/tec

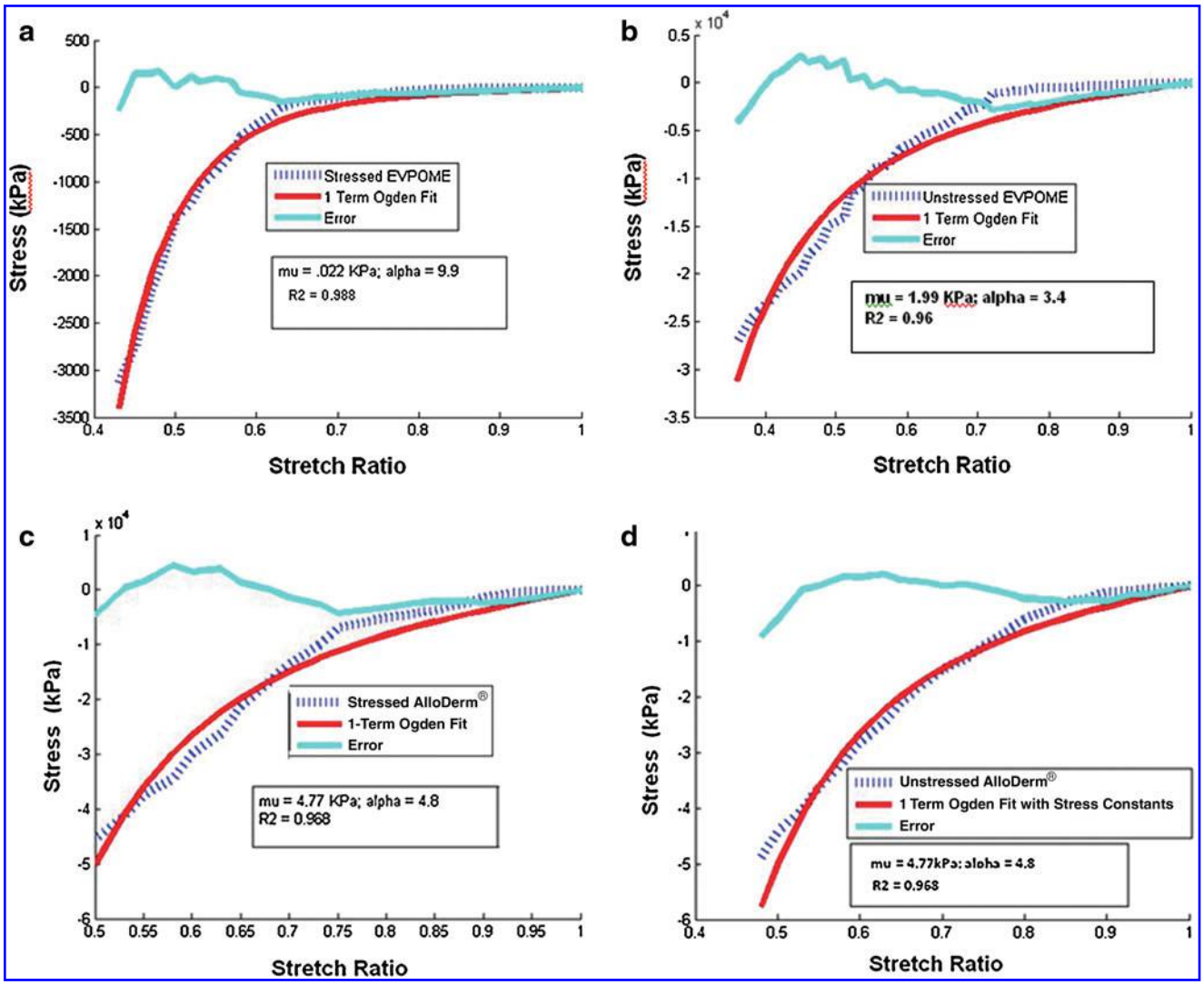

FIG. 7. 1-term Ogden fitting models comparing the stress-to-stretch ratios between stressed and unstressed EVPOMEs **(a** and **b)** and the stressed unstressed AlloDerm **(c** and **d)**. Included are the ratios, the 1-term Ogden fit, and the degree of error. Color images available online at www.liebertpub.com/tec

mechanics observed when testing porcine palate on the mechanical compressor. EVPOME's stratified layers on the surface demonstrate both lower RMS profiles and lower stiffness characteristics than the AlloDerm scaffold (Figs. 4 and 5, respectively). These warrant examining these same tissue types using the SAM system to analyze which cell layers (or combination of layers) contribute most to such mechanical behavior. Further, it is imperative to understand what specific constituents of the cells and the extracellular matrix contribute to the differences in RMS and stiffness values between the AlloDerm, the stressed EVPOME, and the unstressed EVPOME.

Table 1. Compendium of the Stress–Strain Comparisons Among the EVPOME (Both Unstressed and Stressed) AlloDerm® (Both Unstressed and Stressed)

Specimens	*Stress values at maximum dL/L_o (kPa)*
Unstressed AlloDerm	45458.99
Stressed AlloDerm	45852.13
Unstressed EVPOME	3157.84
Stressed EVPOME	27067.19

EVPOME, *ex vivo* produced oral mucosa equivalent.

Future studies here to test elasticity of the individual layers of the mature EVPOME using the SAM compressor and speckle-tracking methods may delineate what particular properties in the EVPOME's seeded material contributes most to these similarities. These studies must include using SAM and the mechanical compressor to evaluate stress–strain on EVPOME tissues during their development at each successive day to determine at which exact day or days the specimens evolve sufficiently to show the observed changes in the 1-term Ogden model's behavior.

Additional microscopy studies (using acoustic, optical, and possibly transmission electron microscopy) will be applied to analyze which subcellular constituents are present at each day of EVPOME development and how they—either individually or in succession—contribute to the changes in linear elasticity observed.

The high similarity in the Ogden behavior between the EVPOMEs—either stressed or unstressed—suggests that the cellular constituents in the EVPOMEs behave alike regardless of whether they are fully attached to the AlloDerm surface. This finding mandates the use of acoustic microscopy to examine the specimens' elastic properties at each of the layers in the EVPOME (both stressed and unstressed) using the compression data and speckle-tracking methods. Further work here will allow us to analyze which components in the tissues contribute most to the changes in stress–strain models observed.

Acknowledgments

This work was supported through the National Institutes of Health (NIH) Regenerative Sciences Training Grant Number 5T90DK070071 and NIH Grant Numbers R21EY018727, R01 DE13417, and NIH center core (P30) grant, EY007003. National Institutes of Health, Bethesda, MD. 20892. We gratefully acknowledge the NIH Resource Center for Medical Ultrasonic Transducer Technology at the University of Southern California (Los Angeles, CA. 90089) for designing and building the high-frequency transducer used in this study.

Disclosure Statement

No competing financial interests exist.

References

1. Cohn, N.A., Emelianov, S.Y., Lubinski, M.A., and O'Donnell, M. An Elasticity Microscope. Part I: Methods. *IEEE Trans Ultrason Ferroelectric Frequency Control* **44,** 1304, 1997.
2. Cohn, N.A. An elasticity microscope for high resolution imaging of tissue stiffness using 50 MHz Ultrasound. University of Michigan, Ann Arbor, MI, Ph.D. Dissertation. 1997.
3. Hotta, T., Yokoo, S., Terashi, H., and Komori, T. Clinical and Histopathological Analysis of Healing Process of Intraoral Reconstruction with Ex Vivo Produced Oral Mucosa Equivalent. *Kobe J Med Sci* **53,** 1, 2007.
4. Izumi, K., Feinberg, S.E., Iida, A., and Yoshizawa, M. Intraoral grafting of an *ex vivo* produced oral mucosa equivalent: a preliminary report. *Int J Oral Maxillofac Surg* **32,** 188, 2003.
5. Lin, W.C., Chang, C.Y.Y., Shen, Y.Y., and Tsai, H.D. Use of autologous buccal mucosa for vaginoplasty: a study of eight cases. *Hum Reprod* **18,** 604, 2003.
6. Barr, R.J., White, G.M., Jones, J.P., Shaw, L.B., and Ross, P.A. Scanning Acoustic Microscopy of Neoplastic and Inflammatory Cutaneous Tissue Specimens. *J Invest Dermatol* **96,** 38, 1991.
7. Winterroth, F., Fowlkes, J.B., Kuo, S., Izumi, K., Feinberg, S.E., Hollister, S.J., and Hollman, K.W. High-resolution ultrasonic monitoring of cellular differentiation in an *ex vivo* produced oral mucosal equivalent (EVPOME). Proceedings IEEE bioultrasonics conference, Rome, Italy, 2009.
8. Erkamp, R.Q., Wiggins, P., Skovoroda, A.R., Emelianov, S.Y., and O'Donnell, M. Measuring the Elastic Modulus of Small Tissue Samples. *Ultrason Imaging* **20,** 17, 1998.
9. Cohn, N.A., Emelianov, S.Y., and O'Donnell, M. An Elasticity Microscope. Part II: Experimental Results. *IEEE Trans Ultrason Ferroelectric Frequency Control* **44,** 1320, 1997.
10. Hollman, K.W., Emelianov, S.Y., Neiss, J.H., Jotyan, G., Spooner, G.J.R., Juhasz, T., Kurtz, R.M., and O'Donnell, M. Strain imaging of corneal tissue with an ultrasound elasticity microscope. *Cornea* **21,** 68, 2002.
11. Yoder, J.H., and Elliot, D.M. Nonlinear and anisotropic tensile properties of graft materials used in soft tissue applications. *Clin Biomech* **25,** 378, 2010.
12. Winterroth, F., Hollman, K.W., Kuo, S., Izumi, K., Feinberg, S.E., Hollister, S.J., and Fowlkes, J.B. Examination and characterization of human mucosal tissue differentiation using scanning acoustic microscopy. *Ultrasound Med Biol* **37,** 1734, 2011.
13. Izumi, K., Song, J., and Feinberg, S.E. Development of a tissue-engineered human oral mucosa: from the bench to the bed side. *Cells Tissues Organs* **176,** 134, 2004.
14. Saijo, Y., Tanaka, M., Okawai, H., and Dunn, F. The ultrasonic properties of gastric cancer tissues obtained with a scanning acoustic microscope. *Ultrasound Med Biol* **17,** 709, 1991.
15. Kolios, M.C., Czarnota, G.J., Lee, M., Hunt, J.W., and Sherar, M.D. Ultrasonic Spectral Parameter Characterization of Apoptosis. *Ultrasound Med Biol* **28,** 589, 2002.
16. Kolios, M.C., Taggart, L., Baddour, R.E., Foster, F.S.., Hunt, J.W., Czarnota, G.J., and Sherar, M.D. An investigation of backscatter power spectra from cells, cell pellets, and microspheres. IEEE Ultrason Symp 752, 2003.
17. Lubinski, M.A., Emelianov, S.Y., and Raghavan, K.R. Lateral displacement estimation using tissue incompressibility. *IEEE Trans UFFC* **43,** 247, 1996.
18. Lubinski, M.A., Emelianov, S.Y., and O'Donnell, M. Speckle tracking methods for ultrasonic elasticity imaging using short time correlation. *IEEE Trans UFFC* **46,** 82, 1999.
19. O'Donnell, M., Skovoroda, A.R., and Shapo, B.M. Internal displacement and strain imaging using ultrasonic speckle tracking. *IEEE Trans UFFC* **41,** 314, 1994.
20. Saijo, Y., Miyakawa, T., Sasaki, H., Tanaka, M., and Nitta, S. Acoustic properties of aortic aneurysm obtained with scanning acoustic microscopy. *Ultrasonics* **42,** 695, 2004.
21. Samani A., Bishop J., Luginbuhl C., and Plewes D.B. Measuring the elastic modulus of ex vivo small tissue samples. *Phys Med Biol*.**48,** 2183, 2003.
22. Winterroth, F. Lee, J., Kuo, S. J., Fowlkes, J.B., Feinberg, S.E., Hollister, S.J., and Hollman, K.W. Acoustic microscopy analyses to determine good vs. failed tissue engineered oral mucosa under normal or thermally stressed culture conditions. *Ann Biomed Eng* **39,** 44, 2011.
23. Zuber, M., Gerber, K., and Erne, P. Myocardial tissue characterization in heart failure by real-time integrated backscatter. *Eur J Ultrasound* **9,** 135, 1999.

Address correspondence to:
Frank Winterroth, PhD
Department of Biomedical Engineering
University of Michigan
1101 Beal Ave.
Lurie BME Bldg., No. 2122
Ann Arbor, MI 48109

E-mail: fwinterr@umich.edu

Received: August 1, 2012
Accepted: September 18, 2012
Online Publication Date: November 21, 2012

This article has been cited by:

1. Scott J. Hollister, Maximilian P. Hollister, Sebastian K. Hollister. 2017. Computational modeling of airway instability and collapse in tracheomalacia. *Respiratory Research* **18**:1. . [CrossRef]
2. Kang Kim, William R. Wagner. 2016. Non-invasive and Non-destructive Characterization of Tissue Engineered Constructs Using Ultrasound Imaging Technologies: A Review. *Annals of Biomedical Engineering* **44**:3, 621-635. [CrossRef]
3. Junning Chen, Rohana Ahmad, Wei Li, Michael Swain, Qing Li. 2015. Biomechanics of oral mucosa. *Journal of The Royal Society Interface* **12**:109, 20150325. [CrossRef]
4. Nam Seung Yun, Ricles Laura M., Suggs Laura J., Emelianov Stanislav Y.. 2015. Imaging Strategies for Tissue Engineering Applications. *Tissue Engineering Part B: Reviews* **21**:1, 88-102. [Abstract] [Full Text HTML] [Full Text PDF] [Full Text PDF with Links]
5. Frank Winterroth, Hiroko Kato, Shiuhyang Kuo, Stephen E. Feinberg, Scott J. Hollister, J. Brian Fowlkes, Kyle W. Hollman. 2014. High-Frequency Ultrasonic Imaging of Growth and Development in Manufactured Engineered Oral Mucosal Tissue Surfaces. *Ultrasound in Medicine & Biology* **40**:9, 2244-2251. [CrossRef]